

ARTICLE



A high-fiber diet synergizes with *Prevotella copri* and exacerbates rheumatoid arthritis

Lingjuan Jiang^{1,2,9}, Mengmeng Shang^{1,2,9}, Shengnan Yu^{2,9}, Yudong Liu³, Hui Zhang⁴, Yangzhong Zhou⁵, Min Wang³, Tingting Wang^{1,2}, Hui Li⁶, Zhihua Liu^{7,8}✉ and Xuan Zhang³✉

© The Author(s), under exclusive licence to CSI and USTC 2022

Both preclinical and established rheumatoid arthritis (RA) patients display alterations in the gut microbiome. *Prevotella* spp. are preferentially enriched in a subset of RA patients. Here, we isolated a *Prevotella* strain, *P. copri* RA, from the feces of RA patients and showed that colonization of *P. copri* RA exacerbated arthritis in a collagen-induced arthritis (CIA) model. With the presence of *P. copri* RA colonization, a high-fiber diet exacerbated arthritis via microbial alterations and intestinal inflammation. Colonization of *P. copri* together with a high-fiber diet enabled the digestion of complex fiber, which led to the overproduction of organic acids, including fumarate, succinate and short-chain fatty acids. Succinate promoted proinflammatory responses in macrophages, and supplementation with succinate exacerbated arthritis in the CIA model. Our findings highlight the importance of dysbiosis when evaluating the effects of dietary interventions on RA pathogenesis and provide new insight into dietary interventions or microbiome modifications to improve RA management.

Keywords: Rheumatoid arthritis; Dysbiosis; *Prevotella copri*; High-fiber diet; Microbiota-derived metabolites

Cellular & Molecular Immunology (2022) 19:1414–1424; <https://doi.org/10.1038/s41423-022-00934-6>

BACKGROUND

Rheumatoid arthritis (RA) is a common systemic autoimmune disease caused by the interplay between genetic and environmental factors. Genetic studies on individuals with RA have identified multiple risk loci [1], and accumulating evidence has highlighted a critical role of environmental factors, including the microbiome and diet, in the pathogenesis of RA [2–4].

We have previously reported that alterations in the gut and oral microbiomes are associated with new-onset RA [5]. Compared to those of controls, the gut microbiomes of individuals with early onset or preclinical RA are particularly enriched in *Prevotella copri* [5–7]. Intestinal dysbiosis can alter mucosal immune responses, which may ultimately contribute to the development of inflammatory arthritis [8]. However, the role of *Prevotella* spp. in modulating the balance between health and disease is complex [9]. For instance, a high abundance of *Prevotella* is associated with dietary fiber-induced improvement in glucose metabolism by promoting glycogen storage [10], and human gut-derived *P. histicola* suppressed arthritis through induction of regulatory T cells (Tregs) [11]. In contrast, transplantation of feces enriched in *P. copri* from patients with RA has been found to promote a proinflammatory Th17 response in regional lymph nodes

of arthritis-prone SKG mice [12]. Together, these data implicate a species- or strain-specific effect of *Prevotella* spp. on metabolic or immune modulation.

The diversity and prevalence of *Prevotella* species and strains in the human microbiome are affected by multiple factors, including lifestyle, diet and geography. In fact, *Prevotella* is usually enriched in non-Western populations, likely due to their relatively plant-rich diets [13]. Distinct *Prevotella* spp. bacteria outcompete commensal bacteria for polysaccharides by encoding specific carbohydrate-active enzymes (CAZymes), which allows them to reside in the human gut [14]. In addition to these differences at the species level, genomic analysis of over 1000 genomes of *P. copri* revealed substantial genetic diversity at the strain level, including genes encoding enzymes for utilization of diverse complex carbohydrates [15]. Indeed, different strains of *P. copri* differ in their abilities to breakdown plant polysaccharides and host-derived mucin [16, 17]. For instance, strains from non-Western subjects show a greater potential for complex fiber degradation [13].

The consumption of dietary fibers by gut microbes produces organic acids (OAs), in particular short-chain fatty acids (SCFAs). Fiber fermentation usually exerts beneficial effects on the host, i.e.,

¹Department of Medical Research Center, National Science and Technology Key Infrastructure on Translational Medicine, Peking Union Medical College Hospital; Department of Rheumatology, Beijing Hospital, National Center of Gerontology, Institute of Geriatric Medicine, Chinese Academy of Medical Sciences and Peking Union Medical College, Beijing 100730, China. ²State Key Laboratory of Complex Severe and Rare Diseases, Peking Union Medical College Hospital, Chinese Academy of Medical Sciences and Peking Union Medical College, Beijing 100730, China. ³Department of Rheumatology, Beijing Hospital, National Center of Gerontology, Institute of Geriatric Medicine, Clinical Immunology Center, Chinese Academy of Medical Sciences and Peking Union Medical College, Beijing 100730, China. ⁴Department of Pathology, Peking Union Medical College Hospital, Chinese Academy of Medical Sciences and Peking Union Medical College, Beijing 100730, China. ⁵Department of Internal Medicine, Peking Union Medical College Hospital, Chinese Academy of Medical Sciences and Peking Union Medical College, Beijing 100730, China. ⁶Key Laboratory of Infection and Immunity, Institute of Biophysics, Chinese Academy of Sciences, Beijing 100101, China. ⁷Institute for Immunology, School of Medicine, Tsinghua University, Beijing 100084, China. ⁸Tsinghua-Peking Center for Life Sciences, Beijing 100084, China. ⁹These authors contributed equally: Lingjuan Jiang, Mengmeng Shang, Shengnan Yu. ✉email: zhihualiu@mail.tsinghua.edu.cn; zxpumch2003@sina.com

Received: 17 March 2022 Accepted: 27 September 2022

Published online: 2 November 2022

promoting glucose homeostasis or facilitating an anti-inflammatory milieu in the gut. For instance, succinate from dietary fiber fermentation was identified as a substrate for intestinal gluconeogenesis, a process that maintains glucose homeostasis [18]. However, these fermentation products can also be detrimental in some situations. For instance, the fermentation of dietary soluble fibers by the gut microbiota induces cholestasis, hepatic inflammation and liver cancer in Toll-like receptor 5 (TLR5)-deficient mice [19]. Furthermore, in the context of intestinal inflammation, butyrate production following dietary fermentation has been shown to exacerbate inflammation by increasing NLRP3 activation [20]. Microbiota-derived succinate has been found to promote *Clostridium difficile* infection after antibiotic treatment or motility disturbance [21]. Succinate, which is produced during bacterial fermentation of dietary fiber, has also been reported in association with dysbiosis, as well as in patients with inflammatory bowel disease and in animal models of intestinal inflammation [22]. Thus, the effect of microbial fermentation of fiber on host health, mainly influenced by diet, can be both context dependent and species (strain) dependent.

RA patients and their physicians are often perplexed by what type of diet the patients should follow. A number of studies have implicated the impact of dietary intervention on disease development. The Mediterranean diet, characterized by a high fiber content, has been shown to reduce the risk of cardiovascular disease due to the anti-inflammatory properties of its contents [23]. As such, a few studies have set out to investigate the association between the Mediterranean diet and risk reduction of inflammatory diseases (i.e., RA) [24]. However, epidemiological studies have failed to show a reduction in RA risk or severity in patients on a Mediterranean diet [25, 26]. Intriguingly, the responses to a Mediterranean diet varied substantially among patients [24–26]. It remains unclear whether specific factors (i.e., the gut microbiome) may contribute to this variability. Notably, a fiber-enriched diet produced divergent immune responses in individuals with different baseline microbiota [27]. There are a few studies suggesting that a patient's baseline microbiota is related to response to treatment [5], but baseline microbiota can also be related to response to diet. Diet components may interact with microbes, but there are few, if any, studies evaluating the combined effects. Thus, there is an urgent need to investigate the combinatory effect of diet and microbes on the pathogenesis or treatment options of RA, as such findings will provide rationales for adjusting diet to modulate the gut microbiome to improve RA management. In this study, we, for the first time, provided evidence that the presence of dysbiosis may interfere with the dietary effect of a high fiber content, which in turn exacerbated RA. Our findings may shed light on the complex interplay between dysbiosis and diet in RA management.

MATERIALS AND METHODS

P. copri isolation and genome sequencing

P. copri was isolated from the feces of RA patients with early RA (<1-year disease duration). For the *P. copri* isolate, cells were grown anaerobically (70% N₂, 20% CO₂, and 10% H₂) in PYG medium supplemented with hematin (25 mg/L) and vitamin K1 (10 mg/L) at 37 °C for 2 days. The strain was sequenced on the Illumina HiSeq 2500 2 × 100 bp platform. Short reads were assembled, and the resulting contigs were then aligned to the *P. copri* reference genome (DSM 18205) with Mauve software.

Mice and induction of arthritis

DBA/1J mice were purchased from the Jackson Laboratory. All mice were maintained in a specific-pathogen free (SPF) facility. All studies were approved by the Animal Ethics Committee of Peking Union Medical College Hospital. All experiments were conducted with sex- and age-matched mice. To induce collagen-induced arthritis (CIA) in mice, female DBA/1 J mice (7–8 weeks old) were injected with an emulsion of bovine CII collagen and complete Freund's adjuvant (CFA, Chondrex) containing a

final concentration of 0.5 mg/ml of *M. tuberculosis* by the subcutaneous route. A booster injection with an emulsion of collagen and incomplete Freund's adjuvant (IFA, Chondrex) was administered on Day 21.

Clinical assessment of arthritis

Clinical scoring for arthritis was performed as described previously [28]. The severity of arthritic limbs was scored as follows: 0 = normal, 1 = mild swelling confined to the tarsals or ankle joint, 2 = mild swelling extending from the ankle to the tarsals, 3 = moderate swelling extending from the ankle to the metatarsal joints, and 4 = severe swelling encompassing the ankle and foot or ankylosis of the limb. Then, the clinical score for each mouse was the sum of the scores for each paw.

Bacterial strains and colonization of mice

P. copri RA was grown in PYG medium supplemented with hematin and vitamin K1. *Bacteroides thetaiotaomicron* ATCC 29148 was grown in TSB media with 1% glucose. DBA/1J mice were subjected to collagen-induced arthritis (CIA) and then treated with a cocktail of antibiotics containing metronidazole (1 g/L), neomycin (1 g/L), vancomycin (0.5 g/L), and ampicillin (1 g/L) in drinking water for 7 days (Day 0 to Day 6) after the second immunization. The mice were then provided with regular sterile water for 48 h (Day 7 to Day 8). A total of 10⁸ CFU of *P. copri* or *B. thetaiotaomicron* was administered to each group via oral gavage on Day 9 after the second immunization. Colonization of the microbiota was confirmed by quantitative PCR of specific bacterial genes. Genomic DNA was extracted from *P. copri* and diluted 10, 100, 1000 and 10,000 times to generate a standard curve for qPCR. The total bacterial DNA in feces was extracted, and total DNA concentrations were measured. The *P. copri* DNA concentration in each sample was determined using the standard curve. *P. copri* composition (%) = $\frac{P. copri \text{ DNA concentration}}{\text{Total DNA concentration}} \times 100$. Oligonucleotide sequences are given in Supplementary Table 1.

Histopathology

To assess tissue pathology, limbs and colons were collected and fixed in 4% paraformaldehyde. Histological sections were stained with hematoxylin and eosin (H&E) and scored in a blinded fashion by a pathologist. Histological sections of colons and joints were evaluated as described in Supplementary Table 2.

Cell culture and stimulation

The cell line HEK-blue-TLR4 (Invivogen) was cultured following the manufacturer's instructions. These reporter HEK-Blue hTLR cells stably co-overexpress the human TLR and NF-κB/AP1-inducible SEAP (secreted embryonic alkaline phosphatase) genes. TLR4 activation was indicated by the absorbance of the SEAP reporter. For stimulation experiments, we determined the growth curves of the two bacterial strains. The two bacterial strains were grown to log phase in the same volume of medium and collected at OD₆₀₀ = 0.6. The supernatants were collected and precipitated with trichloroacetic acid (TCA) acetone. The precipitants were resuspended in PBS and prepared for the following experiment. The bacterial cells were washed with PBS, ground with liquid nitrogen, and resuspended in PBS to obtain extracts. HEK-blue-TLR4 cells were stimulated with the bacterial cell extracts and supernatants of the strain *P. copri* RA and the control strain *B. thetaiotaomicron*. LPS (10 ng/ml) from *Escherichia coli* (strain K12) was included as a positive control. Supernatants were collected and detected with the HEK-Blue detection kit (InvivoGen).

Diets and succinate treatments

Custom diets were based on modification to the AIN-93G control diet and were purchased from XieTong Pharmaceutical Bio-Engineering (China). The fiber-containing diet (FCD) was a diet enriched with 2.5% crude fiber and 7.5% fructooligosaccharide. The non-fiber-containing diet (NCD) was devoid of fiber. The composition of the two diets is provided in Supplementary Table 3. Mice were fed with these diets throughout the experiments after the induction of rheumatoid arthritis. For the sodium succinate treatment experiment, the mice were given sodium succinate (0.5%) at Day 9 after the second immunization until the end of the experiment.

Cytokine and immunoglobulin measurement

Serum cytokines were measured by enzyme-linked immunosorbent assay (ELISA) using Mouse IL-6 ELISA Sets (Raybiotech) according to the

manufacturers' protocols. Concentrations of anti-Bovine type II collagen IgG were then measured using ELISA according to the manufacturers' protocols. Total fecal IgA was measured using sandwich ELISA. For total IgA detection, fecal contents were resuspended in 1 ml of PBS and homogenized at 30 Hz for 30 s for 6 cycles and then centrifuged at $12,000 \times g$ for 10 min. The supernatant was collected and assayed for free IgA by ELISA using the Mouse IgA Quantitation Set (Bethyl).

Cell isolation and flow cytometry analysis

MLN cells were isolated as previously described [29]. For Th17-cell subset quantification, isolated immune cells were stimulated with cell stimulation cocktail (BD) for 5 h. The cells were harvested and stained with CD4 (RM4-5, Invitrogen) and IL-17 antibodies (eBio1787, Invitrogen). Flow cytometry was conducted using a BD FACSCelesta Flow Cytometer. The analysis was performed using FlowJo software (Version 9).

SCFA quantification

SCFAs were analyzed as previously described [30] with modifications. Briefly, for each fecal sample, 20-mg aliquots were extracted with 0.2 ml of 50% H₂SO₄ and 0.3 ml of dichloroethane (containing 10 µg/ml acetic acid-d₄), followed by vortex mixing for 1 min. The sample was centrifuged for 20 min at 12,000 rpm and 4°C and kept at -20°C for 30 min. The supernatant fluid was prepared for GC-MS analysis. GC-MS analysis was performed using an Agilent 8890 gas chromatograph system coupled with an Agilent 5977 mass spectrometer. SCFAs were separated on a DB-FFAP capillary column. A 1-µl aliquot of the analyte was injected in split mode (10:1). The initial temperature was kept at 45°C for 2 min, then raised to 180°C at a rate of 10°C/min, then to 180°C at a rate of 15°C/min, then to 240°C at a rate of 40°C/min, and finally held at 240°C for 3 min. The electronic energy was recorded at 70 eV. SCFA quantification was performed by calculating response factors for each SCFA relative to acetic acid-d₄ using the injections of pure standards.

Fecal succinate and fumarate quantification

For the measurement of succinate and fumarate in the cecum of mice or the feces, the samples were quantified as described [31] with modifications. For each sample, 50-mg aliquots were extracted with 0.005 M NaOH containing 5 µg/mL acetic acid-d₄ and derivatized with 1-propanol:pyridine (3:2, v/v) and propyl chloroformate (PCF). The propyl derivatives were extracted twice with hexane and were measured by an Agilent 8890 gas chromatograph system coupled with an Agilent 7010 mass spectrometer. The system utilized an Agilent DB-624 column (15 m × 250 µm × 1.4 µm). A 1-µl aliquot of the analyte was injected in split mode (10:1). The initial temperature was kept at 36°C for 10 min, then raised to 180°C at a rate of 5°C/min, then to 240°C at a rate of 40°C/min, and finally held at 240°C for 5 min. The energy was 70 eV in electron impact mode.

RNA sequencing and analysis

CIA mice, confirmed for the presence of *P. copri* by qPCR and treated with NCD or FCD diet, were used for transcriptome analysis. After sacrificing the mice, the colon of each mouse was collected and cooled with liquid nitrogen. mRNA was extracted and used for RNA-Seq library preparation following the instructions in the Illumina NEBNext Ultra RNA Library Prep Kit. Sequencing was run on an Illumina High Seq-2000. The resulting reads were aligned to the genome with HISAT2 v2.0.5, and gene counts were normalized using FPKM. Differential expression analysis was performed using the DESeq2 R package (1.16.1). Pathway enrichment analyses were performed using the clusterProfiler R package.

16S rDNA gene sequencing and analysis

Total genomic DNA from samples was extracted using a QIAamp PowerFecal Pro DNA Kit for feces (Qiagen) according to the manufacturer's instructions. 16S rRNA genes of distinct regions (16S V3-V4) were amplified using specific primers with barcodes. The mixed amplicons were then sequenced by Illumina PE250. Before 16S rDNA data analysis, raw sequences were filtered, and paired-end reads were merged to tags by FLASH (V1.2.7). All tags were analyzed by scripts of QIIME 1.9.1, USEARCH v7.0.1090, and Vsearch 2.9.0. Specifically, the tags were clustered into operational taxonomic units (OTUs) with a 97% threshold by using UPARSE, and unique representative OTU sequences were obtained. OTU representative sequences were taxonomically classified using SILVA 132 and QIIME v1.9.1. The OTU table was used to calculate the beta diversities

and to obtain taxonomic profiles. Subsequent statistical analysis was performed in R software.

CAZyme analysis in *Prevotella* genomes

Carbohydrate active enzymes (CAZymes) were identified using dbCAN2 [32] version v2.0.6. The results were filtered by the parameter (E-value < 1e-15, coverage > 0.35) based on the HMMER search. Predicted CAZymes were visualized in R version 4.0.2.

Statistical analysis

We analyzed the data with GraphPad Prism version 7 (San Diego, CA, USA). One-way ANOVA test, two-way ANOVA test, the Mann-Whitney test, and *t* tests were used to compare experimental groups. All values are presented in the figures as the mean ± SEM, with **p* < 0.05, ***p* < 0.01, ****p* < 0.001, *****p* < 0.0001, n.s. no significance.

RESULTS

Colonization of CIA mice with the *Prevotella copri* strain isolated from RA exacerbated arthritis

We and other groups have previously shown an increased abundance of *P. copri* in patients with early RA [5, 6]. We isolated a *Prevotella* strain from the mixed feces of RA patients (*P. copri* RA, PC). The strain was sequenced, and high-quality reads were assembled. The resulting contigs were then aligned to the *P. copri* reference genome (DSM 18205) with Mauve software. There were rearrangements and inversions in the genome of PC (Supplementary Fig. 1), suggesting strain-level differences.

To determine whether the newly isolated *P. copri* RA contributes to RA pathogenesis, collagen-induced arthritis (CIA) was induced in DBA/1J mice, followed by colonization with PC after a course of antibiotic treatment (Fig. 1A). As a control, mice were inoculated with *Bacteroides thetaiotaomicron* (BT), a common host symbiotic bacterial strain in the intestine. We assessed the inflammatory profiles of the mice colonized with PC or BT, as well as the mice that received only antibiotic treatment (CON group). As expected, *Prevotella* spp. were detected in the feces of the PC group but not the BT and CON groups, as determined by gel electrophoresis analysis 3 weeks after inoculation (Fig. 1B). The PC group had higher clinical arthritis scores (Fig. 1C) and higher titers of anti-bovine type II collagen IgG than the BT and CON groups (Fig. 1D). The PC group developed more severe joint inflammation, as reflected by the proliferation of the synovial membrane, increased stromal cell density and infiltration of inflammatory cells (Fig. 1E, F).

Given that gram-negative bacterial colonization may lead to LPS-induced inflammation and fecal IgA secretion, to better understand the mechanism by which PC may promote inflammation, we measured serum LPS levels and fecal IgA levels in the PC, BT and CON groups. We found that plasma LPS levels and fecal IgA levels were significantly higher in the PC group than in the BT and CON groups (Fig. 1G, H), suggesting that LPS may mediate, at least in part, the PC-induced inflammatory response. TLR4 is a major receptor for sensing microbial LPS and initiates the inflammatory response. To investigate the involvement of TLR signaling in PC-induced inflammation, we measured TLR4 activation in TLR4-transfected HEK-293 reporter cells treated with extracts and supernatant of PC or BT. The extracts from PC correspondingly displayed a stronger capacity to induce TLR4 signaling than the extracts from BT (Supplementary Fig. 2A). These findings were corroborated by the TLR4 activation reporting assay with supernatants from PC and BT cells (Supplementary Fig. 2B). These data demonstrate that PC is more capable of activating the TLR4 pathway and inducing inflammation.

PC exacerbated arthritis under a high-fiber diet

Since *Prevotella* spp. are highly capable of degrading cellulose and saccharides via hydrolysis and fermentation, resulting in the production of carboxylic acids [13], we next asked whether PC

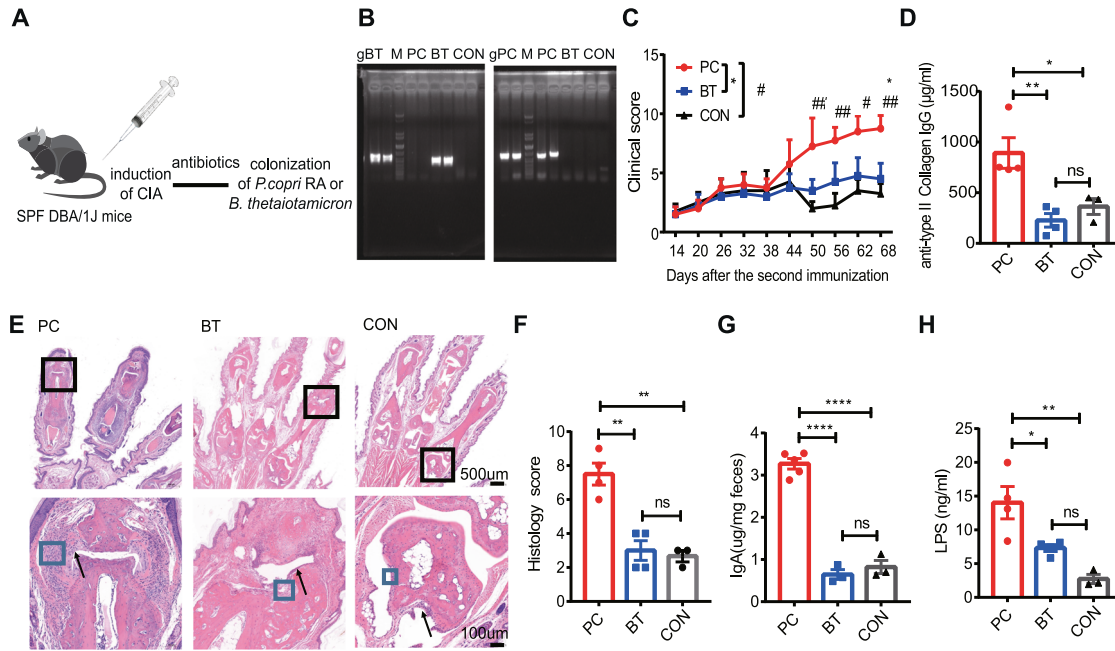


Fig. 1 *P. copri* RA colonization exacerbated arthritis. **A** Illustration of the colonization experiments with *P. copri* RA (PC) and *B. thetaioatamicon* (BT). **B** Confirmation of *P. copri* RA and *B. thetaioatamicon* colonization by agarose gel electrophoresis. gPC indicates *P. copri* genomic DNA (gPC), and *B. thetaioatamicon* genomic DNA (gBT) was used as a positive control; PC, BT, and CON represent total bacterial DNA exacted from the feces of the corresponding group; M, DNA ladder. **C** Clinical scores of collagen-induced arthritis in the PC ($n = 4$), BT ($n = 4$) and CON ($n = 3$) groups. **D** Serum anti-bovine type II collagen IgG level. **E** Representative histology of joints. The black arrow indicates synovial lining-cell hyperplasia, and the blue box indicates stromal cells. **F** Histological scores of joints. **G** Levels of fecal IgA. **H** Serum LPS levels. Each symbol in (**D**, **F**, **G**, and **H**) represents an animal. Error bars indicate the SEM (**C**, **D**, **F**–**H**). P values were determined by two-way ANOVA (**C**), one-way ANOVA (**D**, **F**, **G**, **H**). * $p < 0.05$, ** $p < 0.01$, *** $p < 0.001$, # $p < 0.05$, ## $p < 0.01$, ### $p < 0.001$

aggravates arthritis under a fiber-enriched diet. CIA mice were colonized by oral gavage with 1×10^8 CFUs of PC after a course of antibiotic treatment and then fed a fiber-containing diet (FCD) or a non-fiber-containing diet (NCD) at the same time point as oral gavage (Fig. 2A). PC colonization levels and the consequences of exposure to different dietary interventions were assessed.

The FCD enhanced PC colonization compared to the NCD (Fig. 2B). Furthermore, FCD-fed mice displayed more severe disease characterized by elevated levels of anti-collagen antibodies, higher arthritis scores and greater body weight loss (Fig. 2C–E), as well as more Th17 cells in the mesenteric lymph nodes (MLNs) (Fig. 2F). Notably, FCD-fed mice developed more severe intestinal inflammation manifested as tissue erosion, more infiltration of inflammatory cells, and fewer intestinal crypts than NCD-fed mice (Fig. 2G, H). Histopathological analysis of joints revealed more severe joint damage in FCD-fed mice than in NCD-fed mice, as evidenced by the proliferation of synovial lining cells, pannus formation, and infiltration of inflammatory cells (Fig. 2G, I).

To determine whether PC may contribute to aggravating arthritis through the synergistic effects of diet with dysbiosis in inflammation, CIA mice were colonized by oral gavage with PC or BT and fed an FCD or NCD (Supplementary Fig. 3A). The consequences of PC or BT exposure to different dietary interventions were assessed. *Prevotella* spp. were detected in the feces of the PC but not the BT group, as demonstrated by gel electrophoresis analysis (Supplementary Fig. 3B–C). PC-colonized mice fed the FCD (PC + FCD group) displayed significantly higher arthritis scores and elevated levels of anti-collagen antibodies than PC-colonized mice fed the NCD (PC + NCD group). Moreover, the level of anti-collagen antibody in the PC + FCD group was markedly higher than that in the BT + FCD group (Supplementary Fig. 3D, F). The average body weight of the PC + FCD group was lower than that of the PC + NCD group, but there was no

statistical significance (Supplementary Fig. 3E). The severity of intestinal inflammation in the PC + FCD group was slightly higher than that in the PC + NCD and BT + FCD groups, manifested as more infiltration of inflammatory cells and fewer intestinal crypts, but there were no significant differences (Supplementary Fig. 3G, H). The histology score of the PC + FCD group was significantly higher than that of the PC + NCD group, mainly manifested as the prominent proliferation of synovial lining cells, pannus formation, and massive infiltration of inflammatory cells. The synovial inflammation was slightly more severe in the PC + FCD group than in the BT + FCD group, but there were no significant differences (Supplementary Fig. 3I, J).

The fiber diet plus PC colonization induced inflammation at the transcriptional level

To understand how the FCD synergizing with PC colonization in CIA mice led to more severe inflammation, mRNA sequencing analysis was performed on freshly isolated colon tissues of FCD- and NCD-fed CIA mice colonized with PC. A total of 1444 genes were upregulated and 1487 genes were downregulated in the FCD group compared to the NCD group (Fig. 3A, Supplementary Table 4). Gene Ontology (GO) analysis revealed that the pathways of proinflammatory responses, adaptive immune dysregulation, T-cell activation, and leukocyte differentiation were upregulated in the FCD group (Fig. 3C). Specifically, we observed upregulation of genes involved in T-cell receptor (TCR) signaling, including *Cd4* and *Zap70*, in the FCD group (Fig. 3B), indicating that the FCD may affect T-cell activation and proliferation. The FCD also resulted in the upregulation of *Il18*, *Casp4*, and *Jak3*, as well as *Bcl6* and *Gpr183*, which encode a master regulator of GC B-cell differentiation and an orphan G protein-coupled receptor that is essential for the induction of early plasma blast responses, respectively [33] (Fig. 3B). In accordance with the decreased mucosal thickness

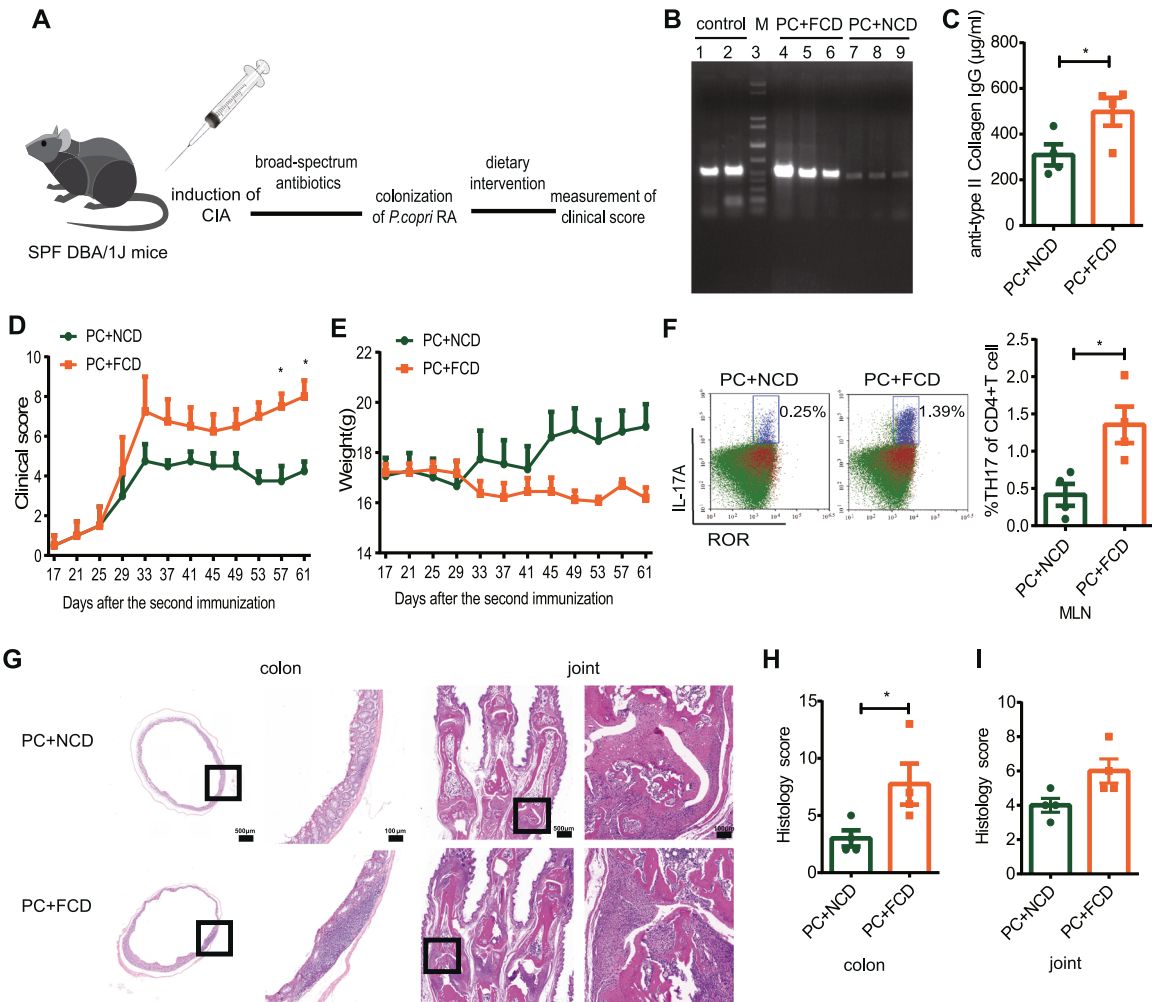


Fig. 2 *P. copri* RA-induced disease severity was promoted by a high-fiber diet. **A** Schematic of CIA mice with dietary intervention. **B** Confirmation of *P. copri* RA colonization by quantitative PCR. Control means *P. copri* genomic DNA; PC + FCD means DNA extracted from FCD group feces; PC + NCD means DNA extracted from NCD group feces. **C** Anti-bovine type II collagen IgG levels in the serum of PC + FCD ($n = 4$) or PC + NCD ($n = 4$) mice. **D** Clinical scores of collagen-induced arthritis. **E** Body weight of mice in the two groups. **F** Flow cytometric analysis of CD4⁺Th17⁺ cells in mesenteric lymph nodes. **G** Histological evaluation of the CIA colon and joint tissues. The scale bar is 100 μ m. **H** The histology scores of the colon tissues. **I** The histology scores of the synovial tissues. Each symbol in (C, F, H, and I) represents an animal. *P* values were determined by two-way ANOVA (D, E), the Mann–Whitney test (F, H, I), and Student's *t* test (C). * $p < 0.05$, ** $p < 0.01$, **** $p < 0.0001$. Abbreviations: PC *P. copri* RA, NCD non-fiber-containing diet, FCD fiber-containing diet

(Fig. 4F), the gene expression levels of mucosal barrier markers (*Muc2* and *Muc6*) and gastrointestinal stem cell markers (*Lgr5*) were significantly decreased in FCD mice. The expression levels of *Mmp3* and *Ctsl*, both of which are implicated in joint destruction in RA [34], were also upregulated in FCD-treated mice (Fig. 3B). Collectively, these observations suggest that FCD intervention in the presence of PC colonization enhances inflammation through increased inflammatory cytokine production, adaptive immunity activation and gut barrier dysfunction.

The fiber-containing diet altered the gut microbiota composition

Given that intestinal inflammation is closely associated with the perturbation of the intestinal microbiota, the effects of a high-fiber diet in the presence of PC colonization on the microbiota composition were investigated. Fecal samples from PC-colonized CIA mice receiving different dietary interventions were collected and subjected to 16S rDNA sequencing. The gut microbial community structure was determined to identify potential pathobionts associated with RA pathogenesis. The FCD group exhibited decreased diversity, expressed in terms of the Shannon

index, compared with that of the NCD group (Fig. 4A). Principal coordinate analysis (PCoA) of the microbial composition based on Bray–Curtis distances was also performed. The analysis showed clear distinctions between NCD and FCD samples (PERMANOVA, $R^2 = 0.64016$, p value = 0.031) (Fig. 4B). Furthermore, the FCD and NCD groups displayed different abundances of the major bacterial phyla in the feces (Fig. 4C). *Firmicutes* and *Bacteroidetes* predominated in the NCD group but not in the FCD group. In contrast, *Akkermansiaceae*, a family within *Verrucomicrobia*, was the most enriched and overrepresented bacterial family in the FCD group (Fig. 4D). Our results were consistent with previous findings that the phylum *Verrucomicrobia* and genus *Akkermansia* were more abundant in RA patients than in controls [35]. A recent study indicated that a high abundance of mucus-degrading *Akkermansiaceae* is a potential risk factor leading to erosion of the colonic mucus layer in sugar-fed wild-type and *Il10*^{-/-} mice, suggesting a role for these bacteria in the pathogenesis of sugar-induced inflammation [36]. In agreement with these findings, the FCD group displayed a reduced mucus layer (Fig. 4F), in accord with the increased levels of *Akkermansiaceae*. On the other hand, the abundance of *Bacteroidaceae* was markedly decreased in the

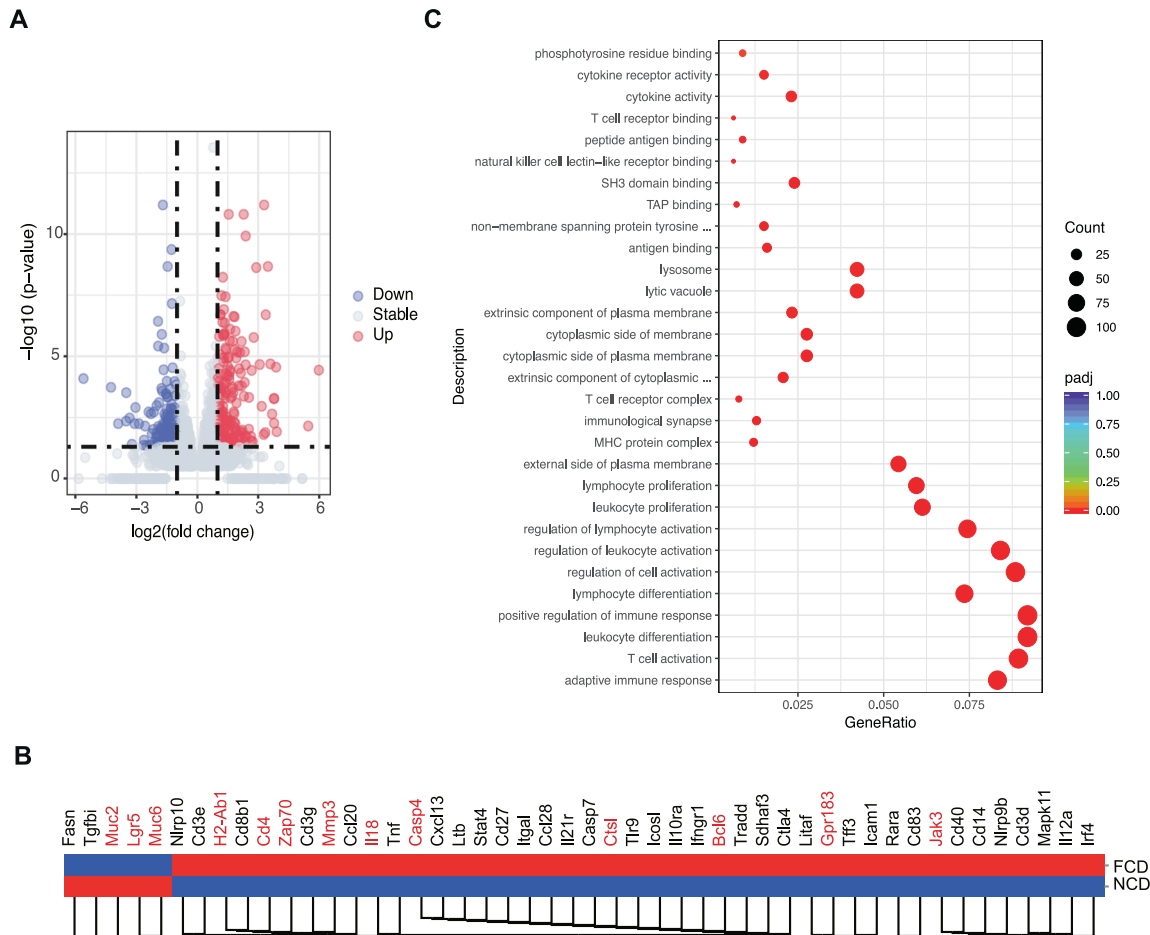


Fig. 3 The impact of dietary intervention on the colon transcriptome. **A** Volcano plots showing the expression of significantly downregulated (blue) and upregulated (red) genes in the FCD and NCD groups. Blue and red dots represent significant DEGs, with the lines denoting a cutoff P value of <0.05 . **B** Heatmap showing the expression of genes involved in the colons of mice subjected to dietary intervention. The red square indicates upregulated genes, and the blue square indicates downregulated genes. For RNA-sequencing data, $n = 4$ per group. Key genes are highlighted in red. **C** Gene Ontology (GO) enrichment analysis among the significantly regulated transcripts from the colons of the FCD and NCD groups

FCD group compared to the NCD group (Fig. 4E), which is consistent with a previous study showing that the relative abundance of *Bacteroides* and *Prevotella* is inversely correlated in the intestine [17]. Taken together, our data indicate that FCD intervention combined with PC colonization led to intestinal dysbiosis characterized by an imbalance between *Akkermansia*-ceae and *Bacteroidaceae*.

PC encodes distinct carbohydrate-active enzymes that might facilitate more efficient fermentation of complex fiber

Given that the FCD differs from the NCD only in fiber content, we evaluated the carbohydrate degradation potential of PC. dbCAN2 (HMMER algorithm) [32] was utilized to predict the CAZymes in PC and the reference genome of *P. copri* DSM 18205. We found that PC encodes more CAZymes than *P. copri* 18205 (Fig. 5A). Specifically, 190 CAZyme-encoding genes were identified in the genome of PC, including 119 glycoside hydrolases (GHs), 42 glycosyltransferases (GTs), 13 carbohydrate esterases, 9 polysaccharide lyases (PLs) and 3 carbohydrate-binding modules (CBMs) (Supplementary Table 5). GH43, GH2 and GH13, which encode β -xylosidases, β -mannosidases and α -amylases, respectively, were the most abundant GH families in PC and *P. copri* 18205 (Fig. 5B).

Comparative analysis of the GH families between the two strains revealed that PC contained a unique set of 17 GHs that were absent in *P. copri* 18205 (Fig. 5B). Of note, rhamnogalacturonan-II (RG-II), comprising endo-aposidase (GH140), DHA hydrolase (GH143), β -l-arabinofuranosidases (GH142 and GH137) and α -galacturonidase (GH138), was identified only in PC (Fig. 5B) but not in *P. copri* 18205. This RG-II degradome was reported to be involved in the degradation of the most structurally complex glycan known [37]. Together, these data illustrate that PC encodes distinct glycan-degrading enzymes, which may give PC an advantage in the utilization and fermentation of complex fiber.

The high-fiber diet skewed the production of inflammatory microbial metabolites

Previous studies have shown that a fiber-rich diet causes the accumulation of metabolites, such as carboxylic acid, in the cecum with concomitant changes in the gut microbiota composition [18]. To evaluate whether FCD aggravates arthritis by enhancing PC degradation of fiber into inflammatory metabolites, we applied a targeted metabolomics approach using GC-MS analysis. We observed significantly higher levels of fumarate, succinate and caproic acid (Fig. 6A, B, G) and significantly lower levels of valeric

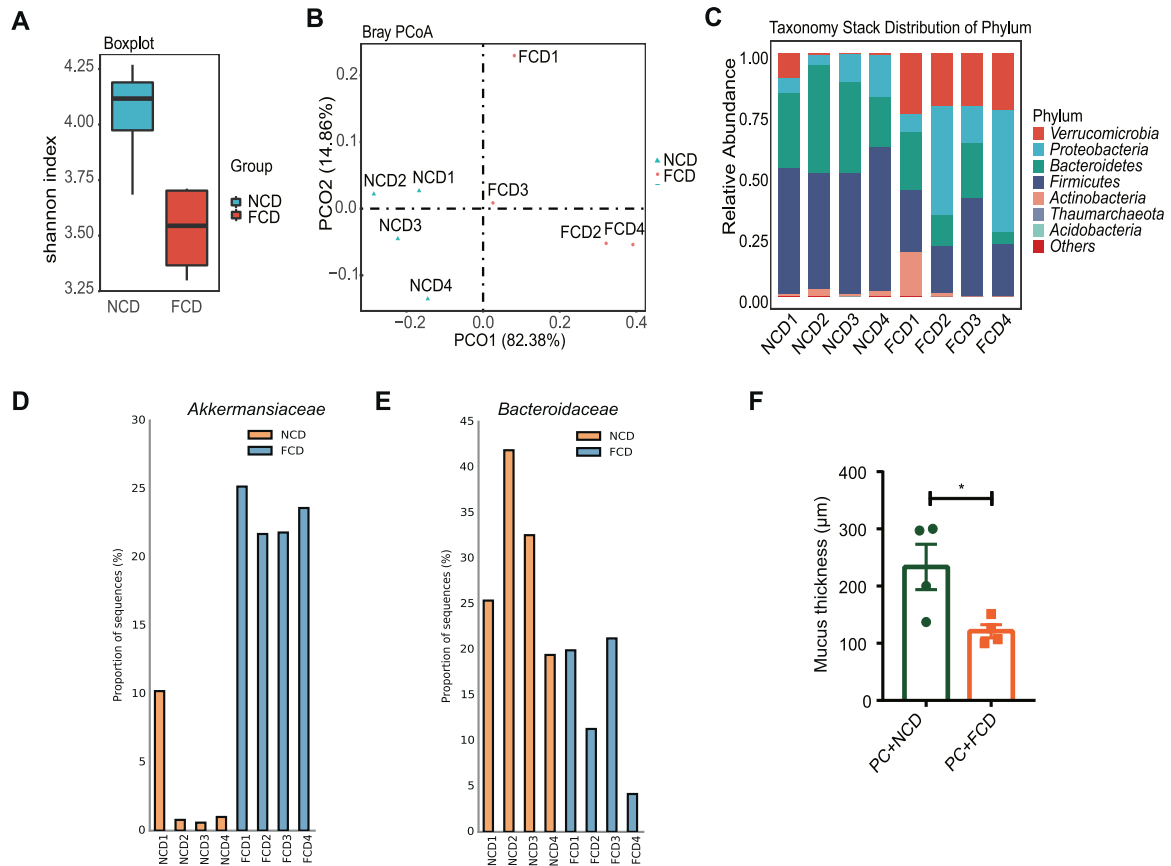


Fig. 4 Dietary intervention affected the gut microbiota colonized with *P. copri* RA. **A** Shannon diversity index between the FCD and NCD groups. (p value = 0.0198). **B** Principal coordinate analysis (PCoA) of the microbial composition based on Bray Curtis. (p value = 0.031, permutational multivariate analysis of variance (PERMANOVA) by Adonis). **C** Taxonomy stack distribution of phyla. **D** Relative abundance of *Akkermansiaceae*. **E** Relative abundance of *Bacteroidaceae*. **F** Mucus layer thickness of the colon. Each symbol in (**F**) represents an animal

acid and heptanoic acid (Fig. 6F, H) in the cecum in FCD-fed mice than in NCD-fed mice. No significant differences in the levels of acetic acid, propionic acid, or butyric acid were identified between the two groups (Fig. 6C–E).

Dietary succinate aggravated arthritis

To assess how the abovementioned microbiota-derived metabolites affected immune responses, we isolated bone marrow-derived macrophages (BMDMs) from DBA/1J mice and tested IL-1 β production by LPS-stimulated BMDMs treated with these metabolites. Succinate has been shown to be a proinflammatory mediator that promotes IL-1 β production [38]. Consistent with these findings, we observed that succinate and fumarate enhanced LPS-mediated IL-1 β production in BMDMs (Fig. 6I). In contrast, other SCFAs, including acetate, propionate, pentanoate, hexanoate and heptylate, suppressed LPS-induced IL-1 β production in BMDMs (Fig. 6I). Together, these results suggest that in the presence of PC, the arthritis of FCD-fed mice was exacerbated by the production of more proinflammatory metabolites but fewer anti-inflammatory metabolites.

To determine whether succinate contributes to the development of RA, we fed CIA mice sodium succinate in drinking water (Fig. 6J). The succinate-fed group displayed a stronger proinflammatory response than the control, as determined by a higher clinical arthritis score (Fig. 6K) and elevated anti-collagen antibody and IL-6 levels (Fig. 6L, M). To identify the pathways involved in succinate supplementation, mRNA sequencing was performed. Intestinal transcriptomes revealed that succinate supplementation increased the expression of genes associated with a

proinflammatory phenotype, such as membrane receptors (i.e., *Ccr7*), nitric oxide synthase 2 (*Nos2*), and chemokines (i.e., *Ccl20*) (Fig. 6N). In addition, succinate treatment affected the expression of genes involved in apoptosis, such as *Bax* and *Mapk3* (Fig. 6N). Taken together, these data suggest that succinate plays a pathogenic role in the development of RA.

DISCUSSION

Prevotella spp., in particular *P. copri*, are preferentially enriched in a subset of RA patients. When we colonized a *P. copri* strain isolated from the feces of RA patients (PC) to create a model of dysbiosis, we showed that an FCD promoted the development of RA through the skewed production of proinflammatory over anti-inflammatory metabolites by PC. The presence of PC enabled the digestion of complex fiber, which led to the production of proinflammatory metabolites, such as succinate, that contributed to RA pathogenesis. Our findings highlight that a high-fiber diet may synergize with dysbiosis in contributing to RA pathogenesis.

The presence and overexpansion of *Prevotella* spp. in the gut microbiome have been associated with detrimental outcomes on human health [6, 7, 10, 18]. Pianta *et al.* reported that a subgroup of RA patients displayed an aberrant immune response to *P. copri*, suggesting that *P. copri* is relevant to immune dysregulation in RA pathogenesis [39]. In this study, we demonstrated the pathogenic role of PC in a CIA model. We found that colonization with PC promoted the development of arthritis, characterized by elevated levels of anti-bovine type II collagen IgG and more severe joint inflammation, which were associated with higher levels of LPS.

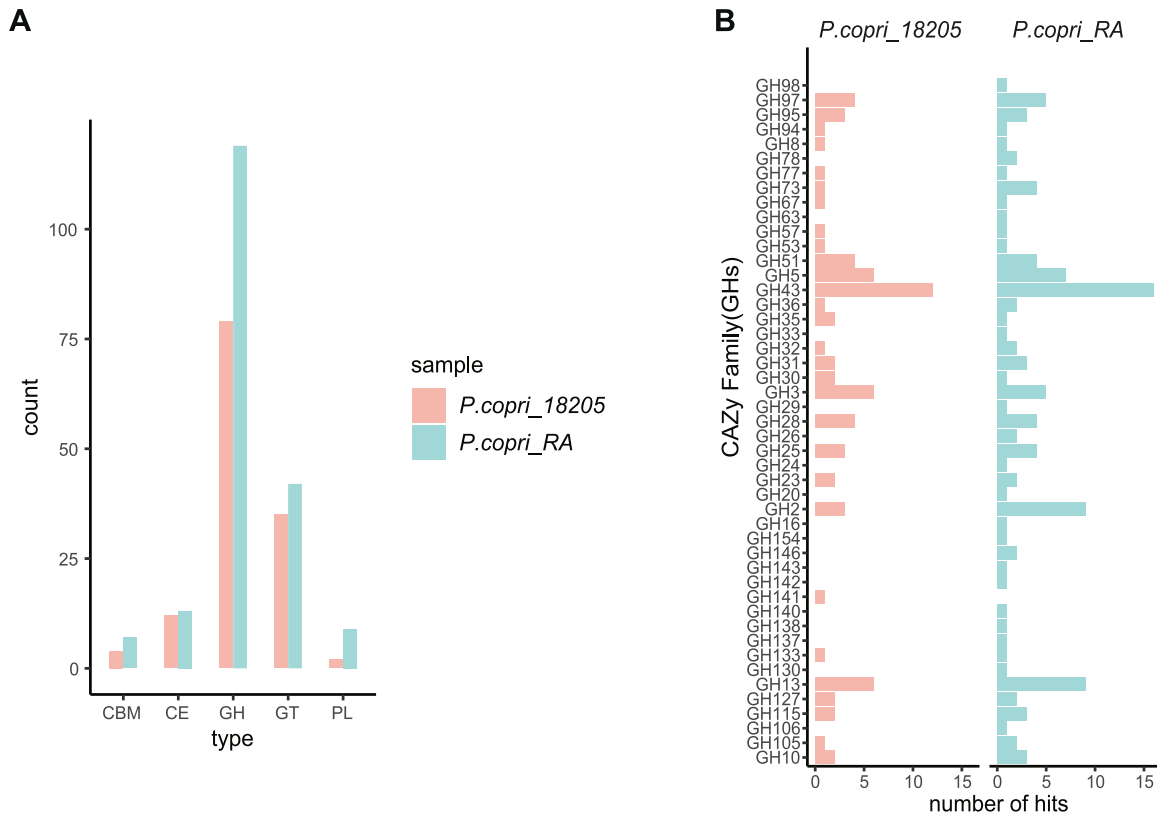


Fig. 5 Unique carbohydrate-active enzyme (CAZyme) classes in the *P. copri* RA strain compared with *P. copri* 18205. **A** The distribution of CAZyme classes in *P. copri* 18205 and *P. copri* RA. **B** Presence or absence of glycoside hydrolases (GHs) in *P. copri* 18205 vs. *P. copri* RA. Differentially encoded GHs are listed. Abbreviations: CBM carbohydrate binding module, CE carbohydrate esterase, GH glycoside hydrolase, GT glycosyltransferase, PL polysaccharide lyase

Furthermore, we showed that PC had a greater capacity to activate the TLR4 pathway, which may contribute to the enhanced immune response. Of interest, we recently reported that *P. copri* was also enriched in patients with ankylosing spondylitis (AS) [40], suggesting that different inflammatory arthritis diseases may share some common microbial signatures.

Dietary fiber intake has been considered to provide health benefits [41]. In this study, we tested the effect of a fiber diet on the development of RA. We introduced PC into the gut microbiota to mimic dysbiosis in RA patients. Intriguingly, we found that PC + FCD mice developed more severe clinical phenotypes than PC + NCD mice, with more severe intestinal inflammation and more pronounced intestinal microbiota perturbation. To further demonstrate whether PC contributes to the effect of diet, we also included BT-colonized mice receiving different diets. We found that the anti-type II collagen antibody in the serum of PC + FCD mice was markedly higher than that of BT + FCD mice, which confirmed that the synergistic effect of PC and FCD may aggravate arthritis. In the human colon, cellulose from dietary fiber is far more digestible than purified crystalline cellulose [42]. Cellulolytic bacteria (i.e., succinate-producing *Prevotella* spp.) are able to degrade polysaccharides to produce different breakdown products [43]. Different *P. copri* isolates can utilize distinct sets of polysaccharides from the diet due to their genomic diversity [17]. In this study, we found that PC, a strain isolated from RA patients, possessed some unique features, such as its expression of rhamnolacturonan-II degradation-related enzymes, which allowed it to digest the most difficult-to-metabolize glycan in the human diet [37]. Thus, in the presence of an FCD, PC can metabolize more fiber into proinflammatory metabolites such as fumarate and succinate.

Nunns et al. showed that the levels of fumarate and succinate were significantly elevated in trauma patients who developed acute respiratory distress syndrome (ARDS) compared to those who did not, suggesting their involvement in inflammatory lung injury [44]. We demonstrated that succinate and fumarate synergized with LPS to promote BMDM production of IL-1 β . We further showed that succinate supplementation exacerbated disease severity in an animal model of RA. In patients with RA, succinate is abundantly present in synovial fluids, and these fluids elicit IL-1 β release from macrophages [45]. Thus, in the context of dysbiosis (i.e., overrepresentation of PC), an FCD can lead to more severe RA due to the excessive production of succinate and fumarate.

In the presence of PC, the FCD promoted microbial imbalances, characterized by an increased abundance of *Akkermansiaceae* and a decreased abundance of *Bacteroidaceae*. Of interest, our results recapitulated some of the features of human RA, as a recent study also demonstrated that RA patients had a higher abundance of *Akkermansia* and a lower abundance of *Bacteroides* [46]. Consistent with our findings, Lam et al. reported that a high-fiber diet favored colonization by *Akkermansia*, which led to the induction of type I interferon signaling and augmented dendritic cell counts [47]. The inflammatory role of *Akkermansia* was also confirmed by Fan et al., who showed that *Akkermansia* could induce an M1-like macrophage response [48]. In addition to stimulating the innate immune response, *Akkermansia* can induce the production of IgG1 antibodies and initiate antigen-specific T-cell responses in mice [49]. We also previously showed that the *A. muciniphila* abundance correlated with inflammation in systemic lupus erythematosus (SLE) patients [50]. Further mechanistic studies are warranted to determine the mechanisms by which *Akkermansia* contributes to

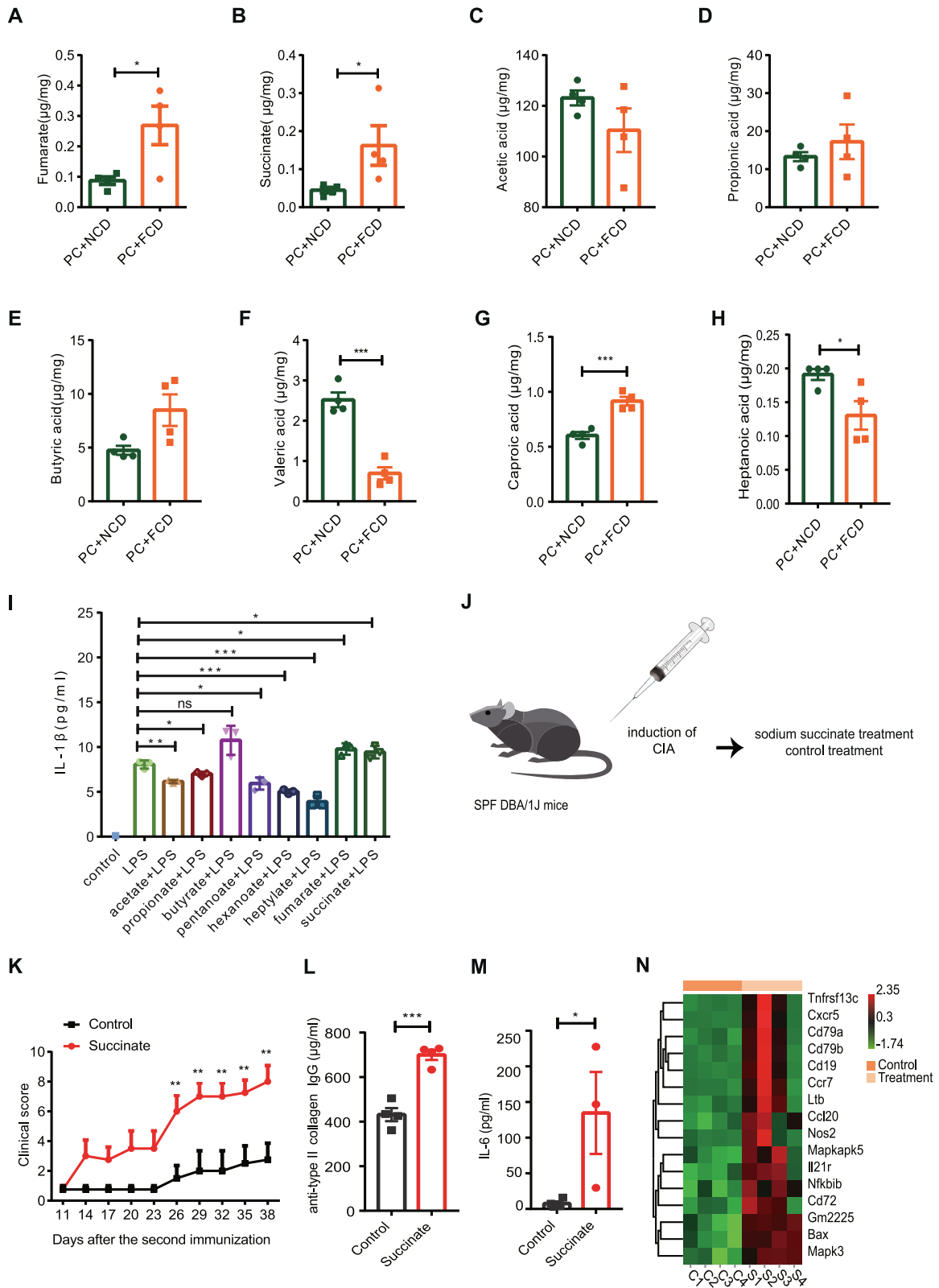


Fig. 6 High-fiber diet with *P. copri* RA colonization induced overproduction of inflammatory microbial metabolites and contributed to RA development. **A, B** The levels of fumarate and succinate in cecal samples. **C–H** Cecum SCFA levels. Error bars indicate the SEM (**A–H**). **I** The level of IL-1β in LPS-stimulated BMDMs pretreated with the designated acids. **J** Schematic of the sodium succinate treatment. **K** Clinical scores of collagen-induced arthritis in the succinate group ($n = 4$) and control group ($n = 4$). **L** Anti-bovine type II collagen IgG levels in serum. **M** Serum IL-6 levels. **N** Heatmap showing the expression of genes involved in the colon of mice subjected to sodium succinate treatment and control treatment. Each symbol in (**A–H**, **L**, and **M**) represents each animal. Error bars indicate the SEM. P values were determined by two-way ANOVA (**K**), and t test (**A–I**, **L**, **M**). * $p < 0.05$, ** $p < 0.01$, *** $p < 0.001$, **** $p < 0.0001$

RA pathogenesis. Taken together, these findings suggest that an FCD together with PC colonization promotes dysbiosis through the alteration of the microbiota composition, which has profound systemic effects and in turn promotes RA development.

A Mediterranean diet has been considered anti-inflammatory and to thus potentially exert a protective role in RA. However, prior work has suggested that a Mediterranean diet may be effective in only a subset of RA patients [51]. The mechanisms underlying the different effects of a Mediterranean diet on RA remain poorly understood but appear to be related to dysbiosis. Our results provide a potential explanation for the variation in response and suggest that specific gut microbiome signatures may be an important determinant of responses to different dietary interventions.

Our results suggested that dysbiosis mediates the effect of the FCD on RA development. Defining the mechanisms by which various dietary interventions influence RA in the context of existing dysbiosis is an important goal with clear clinical implications, especially in personalized medicine. Our study also provides an opportunity to explore potential biomarkers that could have predictive value in assessing the responses to a certain dietary intervention.

DATA AVAILABILITY

The genome sequences and RNA sequence data produced in this study are available at the Sequence Read Archive of the National Center for Biotechnology Information (the accession numbers for the sequences reported in this paper are NCBI SRA: SRR14576269).

REFERENCES

- Raychaudhuri S, Sandor C, Stahl EA, Freudenberg J, Lee HS, Jia X, et al. Five amino acids in three HLA proteins explain most of the association between MHC and seropositive rheumatoid arthritis. *Nat Genet.* 2012;44:291–6. <https://doi.org/10.1038/ng.1076>.
- Scher JU, Abramson SB. The microbiome and rheumatoid arthritis. *Nat Rev Rheumatol.* 2011;7:569–78. <https://doi.org/10.1038/nrrheum.2011.121>.
- Bang SY, Lee KH, Cho SK, Lee HS, Lee KW, Bae SC. Smoking increases rheumatoid arthritis susceptibility in individuals carrying the HLA-DRB1 shared epitope, regardless of rheumatoid factor or anti-cyclic citrullinated peptide antibody status. *Arthritis Rheum.* 2010;62:369–77. <https://doi.org/10.1002/art.27272>.
- Guerreiro CS, Calado A, Sousa J, Fonseca JE. Diet, microbiota, and gut permeability—the unknown triad in rheumatoid arthritis. *Front Med (Lausanne).* 2018;5:349. <https://doi.org/10.3389/fmed.2018.00349>.
- Zhang X, Zhang D, Jia H, Feng Q, Wang D, Liang D, et al. The oral and gut microbiomes are perturbed in rheumatoid arthritis and partly normalized after treatment. *Nat Med.* 2015;21:895–905. <https://doi.org/10.1038/nm.3914>.
- Scher JU, Sczesnak A, Longman RS, Segata N, Ubeda C, Bielski C, et al. Expansion of intestinal *Prevotella copri* correlates with enhanced susceptibility to arthritis. *eLife.* 2013;2:e01202. <https://doi.org/10.7554/eLife.01202>.
- Alpizar-Rodriguez D, Lesker TR, Gronow A, Gilbert B, Raemy E, Lamacchia C, et al. *Prevotella copri* in individuals at risk for rheumatoid arthritis. *Ann Rheum Dis.* 2019;78:590–3. <https://doi.org/10.1136/annrheumdis-2018-214514>.
- Jubair WK, Hendrickson JD, Severs EL, Schulz HM, Adhikari S, Ir D, et al. Modulation of inflammatory arthritis in mice by gut microbiota through mucosal inflammation and autoantibody generation. *Arthritis Rheumatol.* 2018;70:1220–33. <https://doi.org/10.1002/art.40490>.
- Tett A, Pasolli E, Masetti G, Ercolini D, Segata N. *Prevotella* diversity, niches and interactions with the human host. *Nat Rev Microbiol.* 2021. <https://doi.org/10.1038/s41579-021-00559-y>.
- Kovatcheva-Datchary P, Nilsson A, Akrami R, Lee YS, De Vadder F, Arora T, et al. Dietary fiber-induced improvement in glucose metabolism is associated with increased abundance of *Prevotella*. *Cell Metab.* 2015;22:971–82. <https://doi.org/10.1016/j.cmet.2015.10.001>.
- Marietta EV, Murray JA, Luckey DH, Jeraldo PR, Lamba A, Patel R, et al. Suppression of inflammatory arthritis by human gut-derived *Prevotella histicola* in humanized mice. *Arthritis Rheumatol.* 2016;68:2878–88. <https://doi.org/10.1002/art.39785>.
- Maeda Y, Kurakawa T, Umamoto E, Motooka D, Ito Y, Gotoh K, et al. Dysbiosis contributes to arthritis development via activation of autoreactive T cells in the intestine. *Arthritis Rheumatol.* 2016;68:2646–61. <https://doi.org/10.1002/art.39783>.
- De Filippis F, Pasolli E, Tett A, Tarallo S, Naccarati A, De Angelis M, et al. Distinct genetic and functional traits of human intestinal *Prevotella copri* strains are associated with different habitual diets. *Cell Host Microbe.* 2019;25:444–53 e443. <https://doi.org/10.1016/j.chom.2019.01.004>.
- Gálvez EJC, Iljazovic A, Amend L, Lesker TR, Renault T, Thiemann S, et al. Distinct polysaccharide utilization determines interspecies competition between intestinal *Prevotella* spp. *Cell Host Microbe.* 2020;28:838–52 e836. <https://doi.org/10.1016/j.chom.2020.09.012>.
- Tett A, Huang KD, Asnicar F, Fehlner-Peach H, Pasolli E, Karcher N, et al. The *Prevotella copri* complex comprises four distinct clades underrepresented in Westernized populations. *Cell Host Microbe.* 2019;26:666–79 e667. <https://doi.org/10.1016/j.chom.2019.08.018>.
- Wright DP, Rosendale DL, Robertson AM. *Prevotella* enzymes involved in mucin oligosaccharide degradation and evidence for a small operon of genes expressed during growth on mucin. *FEMS Microbiol Lett.* 2000;190:73–9. <https://doi.org/10.1111/j.1574-6968.2000.tb09265.x>.
- Fehlner-Peach H, Magnabosco C, Raghavan V, Scher JU, Tett A, Cox LM, et al. Distinct polysaccharide utilization profiles of human intestinal *Prevotella copri* isolates. *Cell Host Microbe.* 2019;26:680–90.e685. <https://doi.org/10.1016/j.chom.2019.10.013>.
- De Vadder F, Kovatcheva-Datchary P, Zitoun C, Duchamp A, Bäckhed F, Mithieux G. Microbiota-produced succinate improves glucose homeostasis via intestinal gluconeogenesis. *Cell Metab.* 2016;24:151–7. <https://doi.org/10.1016/j.cmet.2016.06.013>.
- Singh V, Yeoh BS, Chassaing B, Xiao X, Saha P, Aguilera Olvera R, et al. Dysregulated microbial fermentation of soluble fiber induces cholestatic liver cancer. *Cell.* 2018;175:679–94 e622. <https://doi.org/10.1016/j.cell.2018.09.004>.
- Singh V, Yeoh BS, Walker RE, Xiao X, Saha P, Golonka RM, et al. Microbiota fermentation-NLRP3 axis shapes the impact of dietary fibres on intestinal inflammation. *Gut.* 2019;68:1801–1812. <https://doi.org/10.1136/gutjnl-2018-316250>.
- Ferreira JA, Wu KJ, Hryckowian AJ, Bouley DM, Weimer BC, Sonnenburg JL. Gut microbiota-produced succinate promotes *C. difficile* infection after antibiotic treatment or motility disturbance. *Cell Host Microbe.* 2014;16:770–7. <https://doi.org/10.1016/j.chom.2014.11.003>.
- Connors J, Dawe N & Van Limbergen J. The role of succinate in the regulation of intestinal inflammation. *Nutrients.* 2018;11. <https://doi.org/10.3390/nu11010025>.
- Battino M, Forbes-Hernández TY, Gasparri M, Afrin S, Cianciosi D, Zhang J, et al. Relevance of functional foods in the Mediterranean diet: the role of olive oil, berries and honey in the prevention of cancer and cardiovascular diseases. *Crit Rev Food Sci Nutr.* 2019;59:893–920. <https://doi.org/10.1080/10408398.2018.1526165>.
- Petersson S, Philippou E, Rodomar C, Nikiphorou E. The Mediterranean diet, fish oil supplements and Rheumatoid arthritis outcomes: evidence from clinical trials. *Autoimmun Rev.* 2018;17:1105–14. <https://doi.org/10.1016/j.autrev.2018.06.007>.
- Hu Y, Costenbader KH, Gao X, Hu FB, Karlson EW, Lu B. Mediterranean diet and incidence of rheumatoid arthritis in women. *Arthritis Care Res (Hoboken).* 2015;67:597–606. <https://doi.org/10.1002/acr.22481>.
- Ingegnoli F, Schioppo T, Scotti I, Ubiali T, De Lucia O, Murgio A, et al. Adherence to Mediterranean diet and patient perception of rheumatoid arthritis. *Complement Ther Med.* 2020;52:102519. <https://doi.org/10.1016/j.ctim.2020.102519>.
- Wastyk HC, Fragiadakis GK, Perelman D, Dahan D, Merrill BD, Yu FB, et al. Gut-microbiota-targeted diets modulate human immune status. *Cell.* 2021;184:4137–53 e4114. <https://doi.org/10.1016/j.cell.2021.06.019>.
- Brand DD, Latham KA, Rosloniec EF. Collagen-induced arthritis. *Nat Protoc.* 2007;2:1269–75. <https://doi.org/10.1038/nprot.2007.173>.
- Qiu Z, Sheridan BS. Isolating lymphocytes from the mouse small intestinal immune system. *J Vis Exp.* 2018. <https://doi.org/10.3791/57281>.
- Wang Y, Li N, Yang JJ, Zhao DM, Chen B, Zhang GQ, et al. Probiotics and fructo-oligosaccharide intervention modulate the microbiota-gut brain axis to improve autism spectrum reducing also the hyper-serotonergic state and the dopamine metabolism disorder. *Pharm Res.* 2020;157:104784. <https://doi.org/10.1016/j.phrs.2020.104784>.
- Zheng X, Qiu Y, Zhong W, Baxter S, Su M, Li Q, et al. A targeted metabolomic protocol for short-chain fatty acids and branched-chain amino acids. *Metabolomics.* 2013;9:818–27. <https://doi.org/10.1007/s11306-013-0500-6>.
- Zhang H, Yohe T, Huang L, Entwistle S, Wu P, Yang Z, et al. dbCAN2: a meta server for automated carbohydrate-active enzyme annotation. *Nucleic Acids Res.* 2018;46:W95–101. <https://doi.org/10.1093/nar/gky418>.
- Gatto D, Paus D, Basten A, Mackay CR, Brink R. Guidance of B cells by the orphan G protein-coupled receptor EBI2 shapes humoral immune responses. *Immunity.* 2009;31:259–69. <https://doi.org/10.1016/j.immuni.2009.06.016>.
- Ikeda Y, Ikata T, Mishiro T, Nakano S, Ikebe M, Yasuoka S. Cathepsins B and L in synovial fluids from patients with rheumatoid arthritis and the effect of cathepsin B on the activation of pro-urokinase. *J Med Invest.* 2000;47:61–75.

35. Chiang H-I, Li J-R, Liu C-C, Liu P-Y, Chen H-H, Chen Y-M, et al. An association of gut microbiota with different phenotypes in chinese patients with rheumatoid arthritis. *J Clin Med*. 2019;8. <https://doi.org/10.3390/jcm8111770>.
36. Khan S, Waliullah S, Godfrey V, Khan MAW, Ramachandran RA, Cantarel BL, et al. Dietary simple sugars alter microbial ecology in the gut and promote colitis in mice. *Sci Transl Med*. 2020;12. <https://doi.org/10.1126/scitranslmed.aay6218>.
37. Ndeh D, Rogowski A, Cartmell A, Luis AS, Baslé A, Gray J, et al. Complex pectin metabolism by gut bacteria reveals novel catalytic functions. *Nature*. 2017;544:65–70. <https://doi.org/10.1038/nature21725>.
38. Tannahill GM, Curtis AM, Adamik J, Palsson-McDermott EM, McGettrick AF, Goel G, et al. Succinate is an inflammatory signal that induces IL-1 beta through HIF-1 alpha. *Nature*. 2013;496:238–+. <https://doi.org/10.1038/nature11986>.
39. Pianta A, Arvikar S, Strle K, Drouin EE, Wang Q, Costello CE, et al. Evidence of the immune relevance of prevotella copri, a gut microbe, in patients with rheumatoid arthritis. *Arthritis Rheumatol*. 2017;69:964–75. <https://doi.org/10.1002/art.40003>.
40. Zhou C, Zhao H, Xiao XY, Chen BD, Guo RJ, Wang Q, et al. Metagenomic profiling of the pro-inflammatory gut microbiota in ankylosing spondylitis. *J Autoimmun*. 2020;107:102360. <https://doi.org/10.1016/j.jaut.2019.102360>.
41. Anderson JW, Baird P, Davis RH Jr, Ferreri S, Knudtson M, Koraym A, et al. Health benefits of dietary fiber. *Nutr Rev*. 2009;67:188–205. <https://doi.org/10.1111/j.1753-4887.2009.00189.x>.
42. Slavin JL, Brauer PM, Marlett JA. Neutral detergent fiber, hemicellulose and cellulose digestibility in human subjects. *J Nutr*. 1981;111:287–97. <https://doi.org/10.1093/jn/111.2.287>.
43. Flint HJ, Bayer EA, Rincon MT, Lamed R, White BA. Polysaccharide utilization by gut bacteria: potential for new insights from genomic analysis. *Nat Rev Microbiol*. 2008;6:121–31. <https://doi.org/10.1038/nrmicro1817>.
44. Nunns GR, Vigneshwar N, Kelher MR, Stettler GR, Gera L, Reisz JA, et al. Succinate activation of SUCNR1 predisposes severely injured patients to neutrophil-mediated ARDS. *Ann Surg*. 2020. <https://doi.org/10.1097/SLA.0000000000004644>.
45. Littlewood-Evans A, Sarret S, Apfel V, Loesle P, Dawson J, Zhang J, et al. GPR91 senses extracellular succinate released from inflammatory macrophages and exacerbates rheumatoid arthritis. *J Exp Med*. 2016;213:1655–62. <https://doi.org/10.1084/jem.20160061>.
46. Chen Y, Ma C, Liu L, He J, Zhu C, Zheng F, et al. Analysis of gut microbiota and metabolites in patients with rheumatoid arthritis and identification of potential biomarkers. *Aging (Albany NY)*. 2021;13. <https://doi.org/10.18632/aging.203641>.
47. Lam KC, Araya RE, Huang A, Chen Q, Di Modica M, Rodrigues RR, et al. Microbiota triggers STING-type I IFN-dependent monocyte reprogramming of the tumor microenvironment. *Cell*. 2021;184:5338–56.e5321. <https://doi.org/10.1016/j.cell.2021.09.019>.
48. Fan L, Xu C, Ge Q, Lin Y, Wong CC, Qi Y, et al. A muciniphila suppresses colorectal tumorigenesis by inducing TLR2/NLRP3-mediated M1-Like TAMs. *Cancer Immunol Res*. 2021;9:1111–24. <https://doi.org/10.1158/2326-6066.CIR-20-1019>.
49. Ansaldo E, Slayden LC, Ching KL, Koch MA, Wolf NK, Plichta DR, et al. Akkermansia muciniphila induces intestinal adaptive immune responses during homeostasis. *Science*. 2019;364:1179–84. <https://doi.org/10.1126/science.aaw7479>.
50. Chen BD, Jia XM, Xu JY, Zhao LD, Ji JY, Wu BX, et al. An autoimmunogenic and proinflammatory profile defined by the gut microbiota of patients with untreated systemic lupus erythematosus. *Arthritis Rheumatol*. 2021;73:232–43. <https://doi.org/10.1002/art.41511>.
51. Nguyen Y, Salliot C, Gelot A, Gambaretti J, Mariette X, Boutron-Ruault MC, et al. Mediterranean diet and risk of rheumatoid arthritis: findings from the French E3N-EPIC cohort study. *Arthritis Rheumatol*. 2021;73:69–77. <https://doi.org/10.1002/art.41487>.

ACKNOWLEDGEMENTS

We thank all donors who participated in this study.

AUTHOR CONTRIBUTIONS

Conception and design of the study: LJJ, ZHL, and XZ; implementation of in vivo and in vitro experiments: LJJ, MMS and SNY; analysis of 16 S rRNA sequencing data and the transcriptome data analysis: LJJ; statistical analysis: MMS and HZ; critical comments: YDL, YZZ, MW, TTW, XZ and ZHL; drafting of manuscript: LJJ and SNY; final approval of the version of the article to be published: all authors.

FUNDING

This work was supported by the National Natural Science Foundation of China (81788101, 82230060, 81630064, and 81701624), the CAMS Innovation Fund for Medical Sciences (CIFMS) (2021-I2M-1-017, 2021-I2M-1-047, 2021-I2M-1-040, and 2021-I2M-1-016), the Capital's Funds for Health Improvement and Research (2020-2-4019) and the National Key Research and Development Program of China (Grant no. 2018YFE0207300).

COMPETING INTERESTS

The authors declare no competing interests.

ETHICS APPROVAL

All studies reported here were approved by the Institutional Review Board and Animal Care and Use Committee of Peking Union Medical College Hospital (PUMCH).

ADDITIONAL INFORMATION

Supplementary information The online version contains supplementary material available at <https://doi.org/10.1038/s41423-022-00934-6>.

Correspondence and requests for materials should be addressed to Zhihua Liu or Xuan Zhang.

Reprints and permission information is available at <http://www.nature.com/reprints>

Springer Nature or its licensor (e.g. a society or other partner) holds exclusive rights to this article under a publishing agreement with the author(s) or other rightsholder(s); author self-archiving of the accepted manuscript version of this article is solely governed by the terms of such publishing agreement and applicable law.